Modelling and Simulation for InSAR

Lee, S. P., Chan, Y. K., Lim, T. S. and Koo, V. C.
Faculty of Engineering and Technology, Multimedia University, Jalan Ayer Keroh Lama, 75450, Melaka Malaysia, Email: lee.sui.ping.zte@gmail.com, ykchan@mmu.edu.my, tslim@mmu.edu.my, vckoo@mmu.edu.my

Abstract
This paper demonstrates models and simulation methods of interferometry synthetic aperture radar (InSAR). The InSAR models are presented in detail, which includes modelling of radar signal geometry, wrapped phase estimation, and phase map estimation. Furthermore, an error model based on interferometric scale is derived by refering to aforementioned models. To consider the real condition of the return signal echo, Gaussian white noise model is applied into simulation model as noisy phase image generation. Moreover, simulation also take scence into challenging terrain conditions like fringes and spiral. The noise or extreme terrain structure might induce interferometry observation, which may lead to undeterminable phase map. To overcome these issues, we implement the well-known difficult task, which are two-dimensional phase unwrapping, and de-noising algorithm. Simulation models discussed in the paper are not only the powerful tools for surface deformation estimation (or digital elevation map generation), but also useful for advance research on InSAR phase unwrapping.

1. Introduction

Interferometry synthetic aperture radar (InSAR) has been emerged as a popular topography measurement method for geophysical applications i.e. digital elevation map generation and terrain movement investigation. Such remote sensing techniques promise a consistent approach to provide the high resolution and good precision interferometry observations in all-weather condition. A number of excellent overview papers of InSAR concept and its applications have been published. (Rosen et al., 2000) provides a comprehensive InSAR review covering the working theories, major algorithmic steps and its issues . Balmer treats entire SAR processing as inverse problem (Balmer and Hartl, 1998). Thus, he emphasizes on InSAR mathematical imaging models and its statistical studies. By relating InSAR measured data to terrain height, (Richard, 2007) established an InSAR equation based on geometry considerations . He has delivered a clear explanation on the relationship of InSAR measurement and topography elevation. Thus, we have built and simulated an InSAR geometry model based on Richard's perspective of geometry considerations. Phase ambiguity is the central problem of InSAR techniques. Overall, interferometric measured phase are ambiguous by noises, under sampling due to extreme terrain structure, and mathematical ill pose of wrapped phase measurement. Among that, the mathematical-ill circumstance has long been viewed as a typical difficult task. SAR measurement phase is wrapped within $(-\pi, \pi]$, however, the principal phase value that represent length of echo range to terrain surface could be more than thousands radian. The principal phase value recovery job is almost impossible due to non-availability of data recovery necessary information. Such phase value reconstruction task is called as phase unwrapping. Over decades, despite a large number of research efforts have been done, such research problem remains open. Such issue become supporting motive of this research work. The main objective of this research is to develop and demonstrate an appropriate simulation tool for advanced research of 2D phase unwrapping. Modelling and simulation works of InSAR are essential for researchers to gain a better handle on those phase ambiguos conditions. It also enables the investigator to concoct different imaginative models (.i.e. phase unwrapping models) and perform advanced analysis based on its simulated outcomes. Various research works related to InSAR simulation have been conducted by scientists across the world. (Xu and Cumming, 1997) introduced an InSAR data simulation technique by generating SLC image pairs with geometry model and noise model. (Li et al., 2005) proposed an iterative interpolation method to simulate airborne InSAR complex images. (Lin and Yang, 2009) developed a simulation model for distributed satellite-borne InSAR SLC images. However, the simulation methods mentioned above are only focus on radar signal or geometry model, further processing step like absolute phase map

estimation is not taken into consideration. Various commercial and non-commercial InSAR software like GMTSAR, Gamma and Doris are able to complete the further processing steps from above methods (Gens, 1999). However, such InSAR softwares do not cover artificial data simulation. Therefore, we proposed a simulation method, which cover complete InSAR processing steps. The proposed simulation method considers at least two distortion cases (which lead to measurement error) simultaneously while other works consider only one case. In this paper, we have reviewed and compared existing algorithms. Also, we have simulated and compared several terrain conditions by the proposed simulation method. Section 2 introduces the necessary mathematical framework for InSAR processing, which covers geometry modelling of InSAR measurement, wrapped phase estimation, phase map estimation, and noise model (additive Gaussian white noise). Noise reduction methods include multilook and wiener filter are presented. The statistical analysis of interferometric phase is shown by multilook phase distribution based on its coherence coefficient. A two-dimensional phase-unwrapping model is introduced into this section. The proper implementation steps of these models are described in section 3. Also, the simulation parameters and its taken terrain scenes are discussed in this section. Section 4 demonstrates simulation results and analysis. Comparisons with other InSAR software are also made. Section 5 concludes the paper.

2. Modelling of Insar

2.1 Radar Signal Model

During InSAR operation, radar antenna propagates frequency to target area and collect its echo signal for data observation. The coherent radar receiver consists of in-phase (I) and quadrature (Q) channels that lead to I term and Q term of radar measurement. The amplitude A and phase φ of the received echo can be calculated by refer to these I and Q data.

$$A = \sqrt{I^2 + Q^2}$$

Equation 1

$$\varphi = \tan^{-1}\left(\frac{Q}{I}\right)$$

Equation 2

The echo signal can be expressed as complex sinusoids $A \exp \varphi$. The transmitted signal can be written as:

$$S_x(t) = A\, exp[j(2\pi ft + \emptyset_0)], \qquad 0 \le t \le \tau$$

Equation 3

Where f denotes radar frequency,$\emptyset_0$ is initial phase of pulse and τ indicates pulse length. The received signal $\widetilde{Sy}$, is expressed on following equation:

$$\widetilde{S_y}(t) = \widetilde{A}\,\rho\, exp\left\{j\left(2\pi f\left(t - \frac{2R_0}{c}\right) + \emptyset_0\right)\right\}, \quad \frac{2R_0}{c} \le t \le \frac{2R_0}{c} + \tau$$

Equation 4

Where ρ is the complex reflectivity of P_o and we assume ρ is a fixed value. $\widetilde{A}$ is a complex- value that covers amplitude and all radar range factors other than radar cross section σ (since σ is proportional to $|\rho|^2$). Speed of light is indicated by c. The ideal baseband received signal after demodulation can be modelled as below:

$$S_y(t) = \widetilde{A}\,\rho\, exp\left\{-j\frac{4\pi f R_0}{c}\right\}, \ \frac{2R_0}{c} \le t \le \frac{2R_0}{c} + \tau$$
$$= \widetilde{A}\,\rho\, exp\left\{-j\frac{4\pi R_0}{\lambda}\right\}, \ \frac{2R_0}{c} \le t \le \frac{2R_0}{c} + \tau$$

Equation 5

By exploiting the phase of received signal, the measured data sample is defined as equation 6:

$$\emptyset := arg[S_y(t)] = arg(\widetilde{A}) + \arg(\rho) - \frac{4\pi R_0}{\lambda}$$

Equation 6

Where *arg*(.) is the function operating on complex number to return angle value.

2.2 InSAR Geometry Models

Topography measurement can be done by space-borne or air-borne InSAR. Such system can be implemented in two ways which are along –track and across-track. Along track InSAR system require at least two pass operations since it is operated in such a way that one antenna record an aperture image at first pass operation, then following aperture images are recorded after certain timespan using same viewing geometry at another pass operations. Such technique allows the detection of spatial changes of land surface for temporal evolution purpose. The following InSAR equations are derived by referring to Richard's perspective of geometry considerations (Richard, 2007). His geometry figures have been adapted into this paper as figure 1 and figure 2. Figure 1 shows the geometry of a radar antenna located at ground plane (reference plane) coordinate y = 0 and altitude coordinate z = h. x coordinate is normal to the page, therefore it is not shown in the figures.

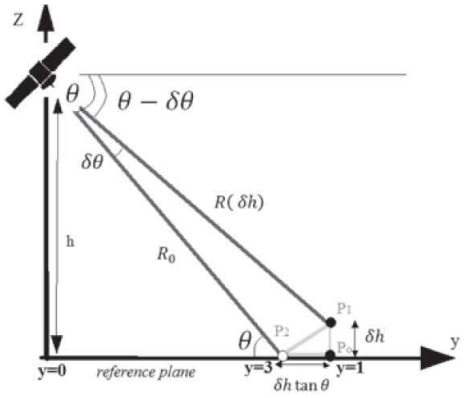

Figure 1: Geometry of along-track InSAR system. This diagram based on figure 5 found in (Richard, 2007)

Po, P1 and P2 indicate positions of scatterer point. For example, Po indicates a position on ground plane z = 0, range dimension y = y1 with grazing angle or depression angle of θ radian. R0 is the range to Po. In geometry model of figure 1, P_1 is elevated by the height of δh from P_0. The variation of relevant height δh is represented by following function:

$$R = R(\delta h) = \sqrt[2]{y^2 + (h - \delta h)^2}$$

$$R(\delta h) = \frac{y_1}{\cos(\theta - \delta\theta)} = \frac{h - \delta h}{\sin(\theta - \delta\theta)}$$

Equation 7

Differential of the function are calculated:

$$\frac{\partial R(\delta h)}{\partial(\delta h)} = \frac{\frac{1}{2}(-2h + 2\delta h)}{\sqrt[2]{y_1^2 + (h - \delta h)^2}} = \frac{(\delta h - h)}{R(\delta h)}$$

Equation 8

By rewriting the differential result in this form, we can relate the range variation respect to height variation.

$$\delta R = -\left(\frac{h - \delta h}{R(\delta h)}\right) \delta h$$

Equation 9

By considering such effect on ground plane as P_0 where z = 0, so δh = 0. It becomes:

$$\delta R = -\left(\frac{h}{R_0}\right) \delta h = -\delta h \sin\theta$$

Equation 10

In this scenario, the measured phase in equation (6) is can be expressed as:

$$\delta\emptyset = -\left(\frac{4\pi}{\lambda}\right) \delta R = \left(\frac{4\pi}{\lambda}\right) \delta h \sin\theta$$

Equation 11

During InSAR processing, the real three dimension world is projected into two dimension plane. Range value of scatterer P_1 is lower than P_0 since the time delay arrived earlier due to its higher location. As a result, ground coordinate of P_1 is located at y_3.

$$y_3 = y_1 - \delta h \tan\theta$$

Equation 12

Equation (11) and (12) shows the single sample of processed phase information with its coordinate in one dimensional line (y-plane). The InSAR systems travel in x-plane, record samples line-by-line and lead to two-dimensional array of phase image formation. Recall equation (6), G(x,y) indicates aperture image of phase information from received signal.

$$G(x,y) = -\left(\frac{4\pi}{\lambda}\right) \delta R(x,y)$$
$$= arg\left[\tilde{A}(x,y)\right] + \arg[\rho(x,y)] - \frac{4\pi R_0}{\lambda}$$

Equation 13

Figure 2 illustrates the geometry model of across-track InSAR system. Across-track InSAR system consists of two antennas separated by a baseline distance B normal to the plane of moving track. $G_1(x,y)$ and $G_2(x,y)$ represent two aperture image information from two antenna of different position. In this system, P_o and P_1 indicates the same target position from apertures of $G_1(x,y)$ and $G_2(x,y)$.The different location of the antenna sensors are lead to a height different of δh. Such principle could be applied for elevation map generation. By refering to figure 2, the different between $G_1(x,y)$ and $G_2(x,y)$ in term of range is B cosθ.

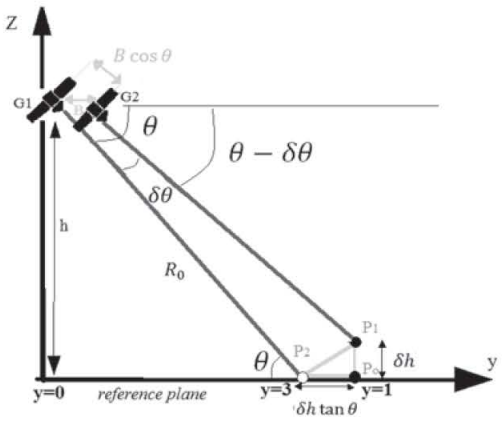

Figure 2: Geometry of across-track InSAR system. This diagram adapted from figure 8 found in (Richard, 2007)

Thus, the phase difference between the two apertures becomes:

$$\emptyset_{G_1G_2}(x,y) = \emptyset_{G_1}(x,y) - \emptyset_{G_1}(x,y)$$
$$\cong -\frac{4\pi}{\lambda} B\cos\theta$$

Equation 14

Differentiating equation 14 with respect to grazing angle gives:

$$\frac{\partial \emptyset_{G_1G_2}}{\partial\theta} = \frac{4\pi}{\lambda} B\sin\theta$$
$$\delta\theta = \frac{\lambda}{4\pi B\sin\theta}\delta\emptyset_{G_1G_2}$$

Equation 15

By referring to the geometry of figure 2, we obtain:

$$\frac{h}{y_1} = \tan\theta$$
$$\frac{h-\delta h}{y_1} = \tan(\theta-\delta\theta)$$
$$\frac{\delta h}{h} = \frac{\tan\theta - \tan(\theta-\delta\theta)}{\tan\theta}$$

Equation 16

Considering δθ as very small, equation 16 can be written as:

$$\frac{\delta h}{h} \cong \frac{\delta\theta}{\tan\theta} = \delta\theta\cot\theta$$
$$\delta h \cong (h\cot\theta)\delta\theta$$

Equation 17

By solving equation 15 and equation 17, we get a topography map of elevation measurement.

$$\delta h(x,y) = \frac{\lambda h\cot\theta}{4\pi B\sin\theta}\delta\emptyset_{G_1G_2}$$

Equation 18

From equation 18, we derive an interferometric scale as $\gamma = \frac{\lambda h\cot\theta}{4\pi B\sin\theta}$. Since the maximum phase variation of $\delta\emptyset_{G_1G_2}$ is 2π, so abrupt change of height among adjacent sample beyond $\dot{h}$ meter will lead to a residue pixel or whole image corruption. Such circumstance is model to equation 19.

$$\dot{h} = 2\pi\gamma$$

Equation 19

It is noted that the radar geometry model is not fully represents real world of SAR data acquisition since SAR issues like backscattering and shadowing are not being taken into consideration. In real circumstance, each resolution element is also constitutes of a lot of arbitrary scatters. Instead of considering InSAR data as mean value of the geometrical point scatterers, we should treat it as imaging process to construct three dimensional terrain structure.

2.3 Wrapped Phase Estimation Model and Its Problem Formulation

During InSAR processing, estimation of phase difference between apertures of SAR images (wrapped phase estimation) is represented by interferogram. Interferogram $I_{G_1G_2}$ can be generated by computing $G_1(x,y)$ multiply conjugate of $G_2(x,y)$, $G_1(x,y)$ and $G_2(x,y)$ are apertures of SAR images.

$$I_{G_1G_2(x,y)=G_1(x,y)\overline{G_2(x,y)}}$$

Equation 20

The phase values extracted via receiver are wrapped in the interval of (-π,π]. However, absolute phase value which represents the range to ground surface can be many radians (Zebker and Lu, 1998). As shown in equation 21, Φ denoted absolute phase. k is number of wavelength and Φ_p stands for principle phase value.

$$\Phi(x,y) = 2\pi k(x,y) + \Phi_p(x,y)$$

Equation 21

The phase difference estimated from equation 20 is not the absolute phase difference (it is wrapped phase difference) due to 2π modulus issue. In addition, extreme terrain structures (e.g fringes) and noise will further corrupt the interferometry measurement. This makes phase determination ambiguous. Thus, two dimensional phase unwrapping (2D- phase unwrapping) to recover unambiguous phase value becomes the key problem of InSAR processing. Strictly saying, data recovery work is an impossible task due to its mathematical ill pose. Literature study reveals that absolute phase can be estimated via interferometry spatial or temporal context (Ghighlia and Pritt, 1998). Thus, this can be estimated based on assumptions.

2.4 Two Dimensional Phase Unwrapping Model

The following equations shows 2D-phase unwrapping model based on Itoh condition (Munther and Francise, 2013).

Such method estimates the differences of the phase at each image point in either images dimension as an approximation to the derivative and integrate the result. Once the discontinuity is detected among adjacent pixel, multiple of 2π will be added or deducted in order to remove the discontinuity. By referring to equation 21, we rewrite the absolute phase determination function where $\emptyset(x,y)$ is the estimate absolute phase value, $\emptyset_w(x,y)$ denoted wrap phase. The number of cycle k is determined by summation of vertical adjustment parameter, $k_v(x,y)$ and horizontal adjustment parameter, $k_h(x,y)$. Δh and Δv denoted the phase difference among adjacent pixel horizontally and vertically, while m and n indicate column and row number of the interferogram.

$$\emptyset(x,y) = \emptyset_w(x,y) + 2\pi\left[\sum_{x=1}^{m} k_v(x,y) + \sum_{y=1}^{n} k_h(x,y)\right]$$

$$k_h(x,y) = \begin{cases} 0\ , \Delta h \le \pi \\ 1\ , \Delta h \ge \pi \cap [\emptyset(x-1,y) > \emptyset(x,y)] \\ -1, \Delta h\ \ge \pi \cap [\emptyset(x-1,y) < \emptyset(x,y)] \end{cases}$$

$$k_v(x,y) = \begin{cases} 0\ , \Delta v \le \pi \\ 1\ , \Delta v \ge \pi \cap [\emptyset(x,y-1) > \emptyset(x,y)] \\ -1, \Delta v\ \ge \pi \cap [\emptyset(x,y-1) < \emptyset(x,y)] \end{cases}$$

$$\Delta h = \emptyset(x,y) - \emptyset(x-1,y)$$
$$\Delta v = \emptyset(x,y) - \emptyset(x,y-1)$$

Equation 22

2.5 Noise Model

In real circumstance, such phase measurements are induced by unknown noise from echo signal. To simulate this scenario, we generate a noisy phase image by adding the complex-value Gaussian white noise $\mathcal{N}(.)$ to the interferogram. Equation 23 show the PDF model of Gaussian white noise where σ stands for variance and $\bar{x}$ indicate mean of input variable (we employed zero- mean Gaussian model, $\bar{x} = 0$).

$$P_G(x) = \frac{1}{\sqrt{2\pi\sigma^2}} exp - \left(\frac{(x-\bar{x})^2}{2\sigma^2}\right)$$

Equation 23

2.6 Noise Reduction Models

In this paper, two- dimensional wiener filter (Matlab help file) is employed as denoising method by estimating the local mean and variance around each pixel.

$$b(x,y) = \mu + \frac{\sigma^2 - v^2}{\sigma^2}(a(x,y) - \mu)$$

Equation 24

where local mean is estimated by refering to nearby adjacent pixels $a(n,m)$within N x M window.

$$\mu = \frac{1}{NM}\sum a(n,m)$$
$$\sigma^2 = \sum a^2(m,n) - \mu^2$$

Equation 25

Another noise reduction method, multilook techniques is also frequently employed to overcome phase noise by averaging neighbouring pixels.

$$z(x,y) = \frac{1}{n}\sum_{i=1}^{n} G_1(x,y)\overline{G_2(x,y)}$$
$$= |z|\exp(i\emptyset)$$

Equation 26

It is noted that $G_1(x,y)$ and $G_2(x,y)$are the pair of complex single look SAR images, n is the number of look. This is a promising technique that Lee have derived following pdf for multilook phase distribution (Lee et al., 1994) (Figure 3):

$$p_\emptyset(\emptyset) = \frac{\Gamma\left(n+\frac{1}{2}\right)(1-|c|^2)^n\beta}{2\sqrt{\pi}\Gamma(n)(1-\beta^2)} + \frac{(1-|c|^2)^n}{2\pi} \cdot F\left(n,1;\frac{1}{2};\beta^2\right),\ -\pi < (\emptyset - \vartheta) < \pi$$

Equation 27

Where $\beta = |c|\cos(\emptyset - \vartheta)$ and F(.) is a hypergeometric function. $\Gamma(.)$is gamma function. The coherence coefficient is defined as follow:

$$c = \frac{E[G_1\overline{G_2}]}{\sqrt{E[{G_1}^2]E[{G_2}^2]}} = |c|\exp(i\vartheta)$$

Equation 28

Where |C| is the coherence and ϑ is the phase of coherence coefficient.

3. Proposed InSAR Simulation Technique

Figure 4 shows the proposed InSAR simulation method. In this simulation, various artificial three-dimensional terrain structures (include fringes, spiral and hill plane) is generated. We also simulate interferometry observed data from different aperture views (G_1 and G_2) by referring to aforementioned radar signal geometry model. The interferogram is generated via computation of the interference pattern caused by the phase difference between two

SAR images acquired from G_1 and G2. The interferogram is an estimation map of wrapped phase difference. Additive complex-valued Gaussian white noise is generated to produce an ambiguous wrapped phase image. In this step, multilook techniques could be implemented to overcome the phase noise and reducing phase unwrapping problem. Then, we implement a 2D phase unwrapping method, i.e., Itoh method for absolute phase map estimation. 2D Wiener filter with 5 x 5 window is employed for de-noising purpose. Finally, terrain height information can be calculated by relating the unwrapped and de-noised outcome as geophysical measurement to radar signal geometry. In this paper, we implemented these simulation steps in two ways, with (4 look) and without multilook (single look) by refer simulation parameter of Table 1.

4. Simulation Result and Comparison Table

4.1 Simulation Result

Proposed simulation techniques are implemented by referring to simulation parameters of Table 1. Such simulations take into consideration of three terrain structure types including terrain hill and sinking whole structure, fringe structure, and spiral structure. As shown in Figure 6, Figure 7 and Figure 8, each set of terrain structure simulation results are organised as follow: first diagram represents relevant artificial terrain structure (or expected outcome). Second result indicates a noisy interferogram after InSAR processing. Then, it follows by reconstruction plots of relevant terrain structure after phase unwrapping and denoising. Such final plotting could be compared with expected outcome (first diagram) for performance evaluation. Figure 6 shows simulation results of terrain hill and sinking hole. We observed that the shape of final simulated result is very close to the expected outcome. In this case, noise is well-suppressed and the phase unwrapping method has well-approximated and reconstructed the terrain structure into proper value. This simulation results shows great performance since all pre-assumptions are well-hold. During fringe simulation in Figure 7, we observe that terrain map is not being reconstructed properly at edge area during Itoh unwrapping. We notice that relevant edge area encounter the abrupt height variation more than 600m.

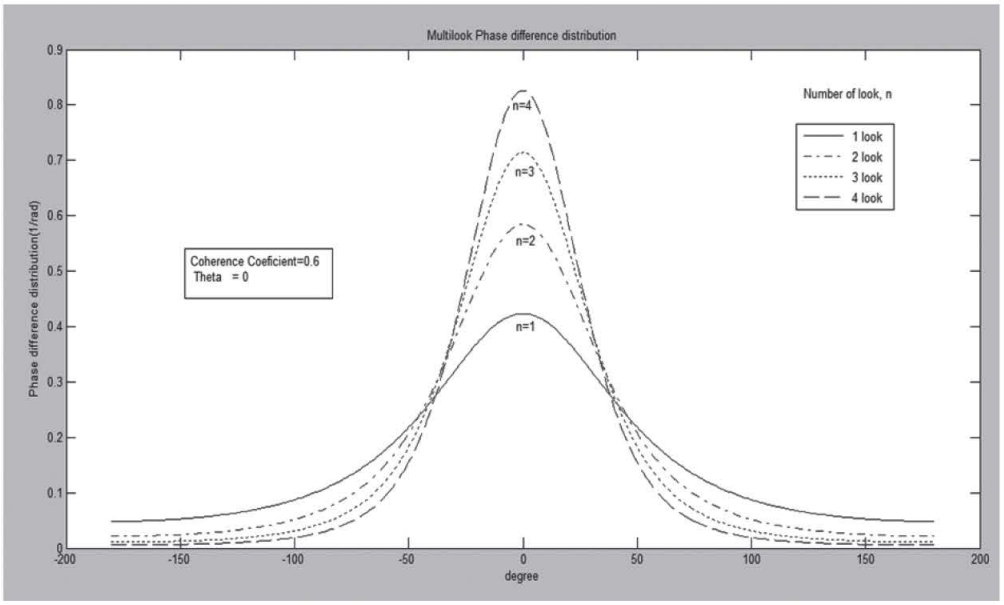

Figure 3: Pdf Plotting of Multilook Phase Distribution (c=0 and ϑ=0)

Table 1: Simulation Parameter

Radar Frequency	10 GHZ(X-band)
Wavelength	0.03m
Antenna Height	5000m
Baseline distance	1m
Grazing Angle	30 degree
Noise Variance	0.4

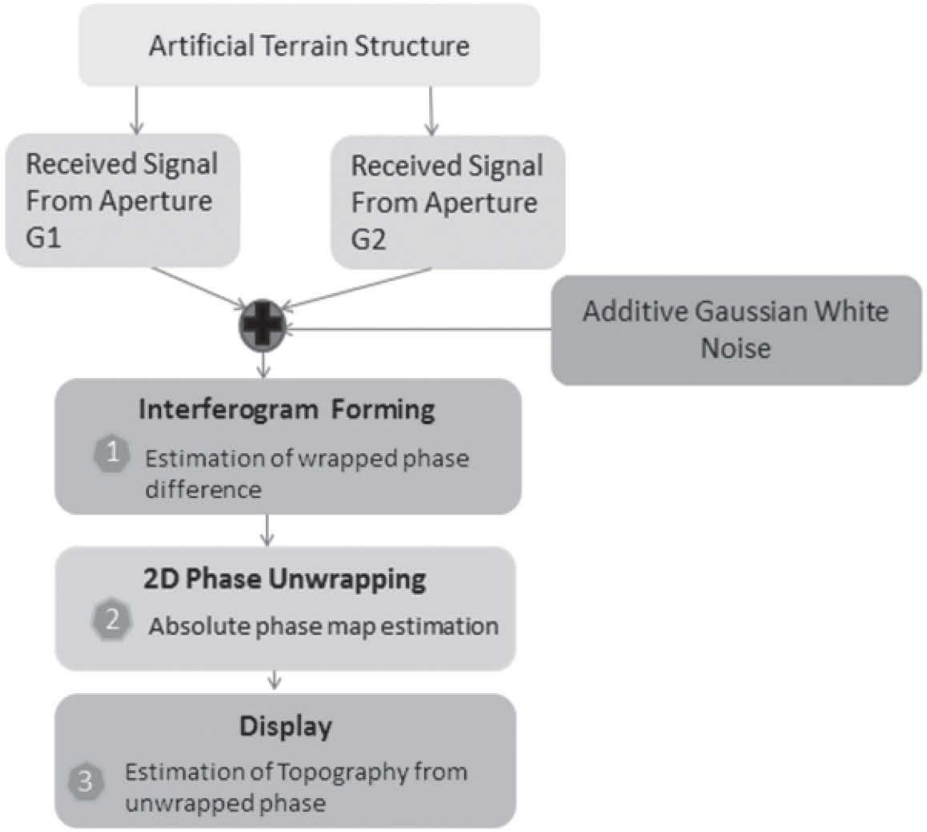

Figure 4: Simulation flow chart for InSAR

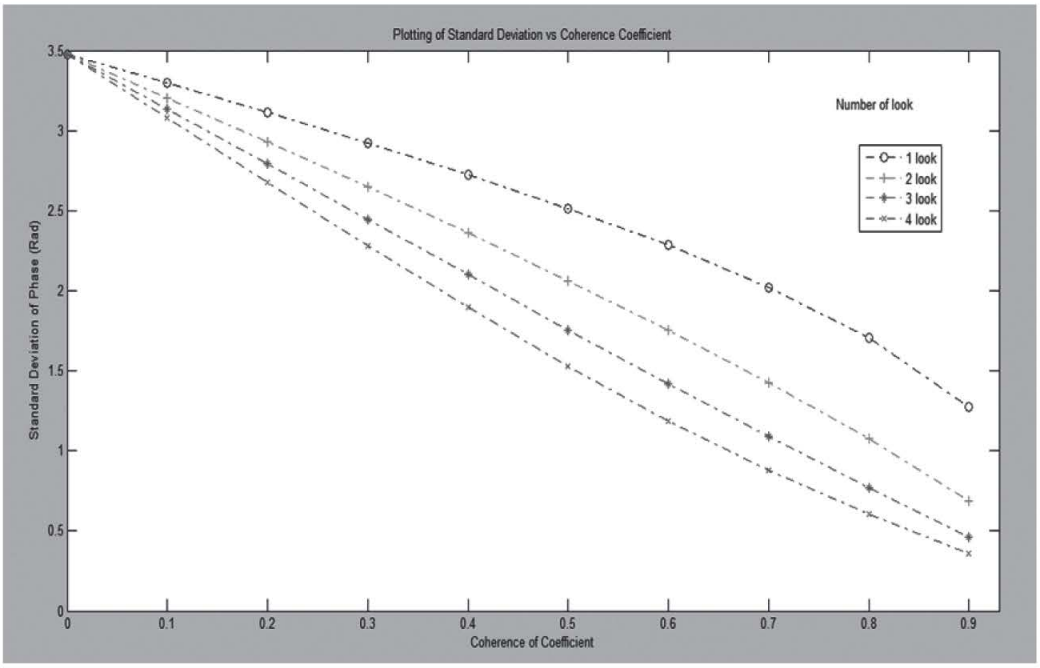

Figure 5: Plotting of interferometric phase vs coherence coefficient

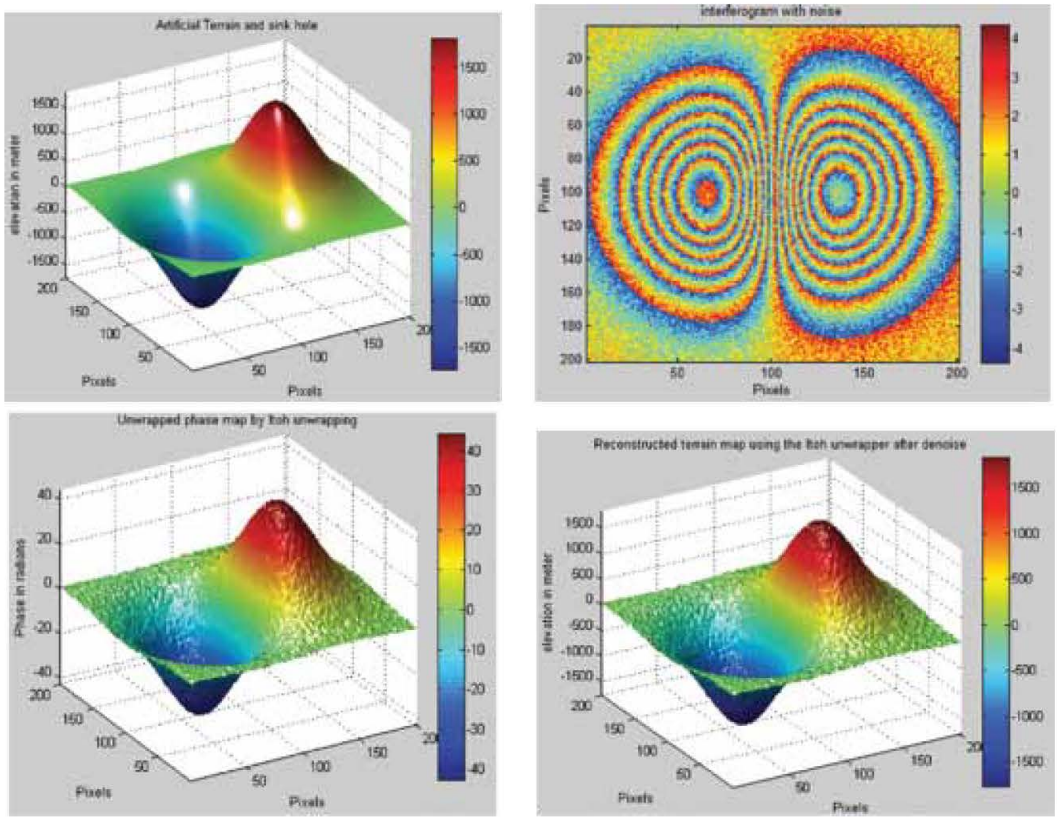

Figure 6: InSAR Simulation of terrain hill & sinking holes

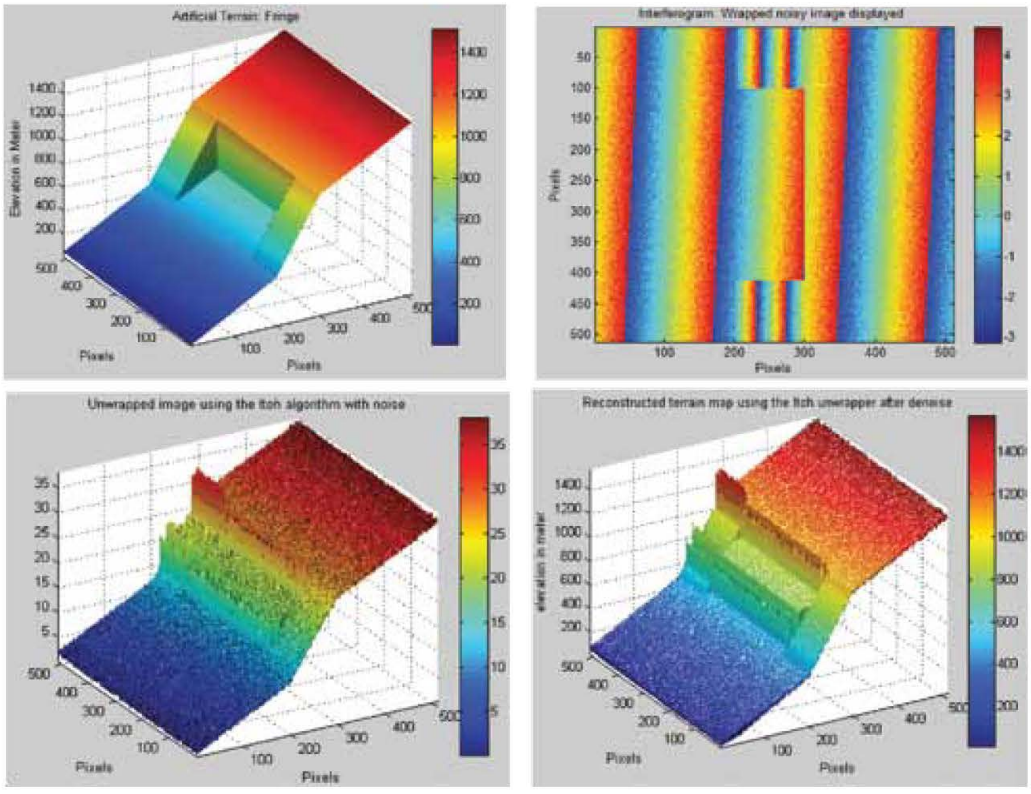

Figure 7: InSAR Simulation of fringe

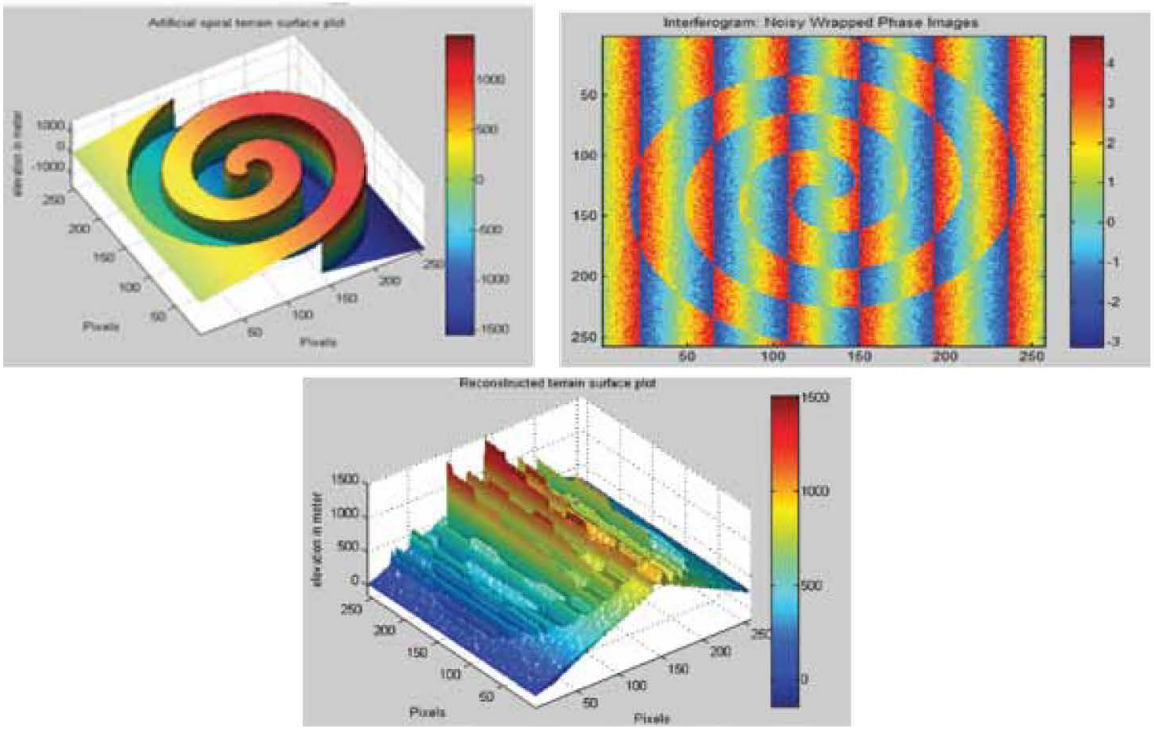

Figure 8: InSAR Simulation of spiral plane

By referring to equation 19, we substituted the simulation parameter and defined our interferometric scale at γ =44.35.The geometry limit of such InSAR system would be $\hat{h}$=44.35 x 2π≈ 260m. In this scenario, the height variation of fringe is far beyond its geometry limit. Thus, final processing outcome offringe structure has reconstructed to a wrong shape at its effected region. Figure 8 shows simulation of spiral plane with a failure final simulated outcome that both Itoh method and wiener filter failed to reconstruct the terrain map of spiral shape. Such spiral plane considered as extreme structure since more than 80 percent of its region encounter height variation beyond the limit. The proposed phase-unwrapping method failed to define the spiral edge since its working principal define the integral path vertically and horizontally while relevant edge shaped spirally. In this scenario, all pre-assumptions are no longer held. Such extreme terrain structures simulations show that the Itoh unwrapping approach allows local errors due to abrupt phase variations beyond interferometric limit, causing errors across full unwrapped terrain image. This solution is sensitive to inconsistencies in wrapped phase, leading to significant errors. Since two-dimensional phase unwrapping is a well-known unsolved issue, advance research could be conducted for extreme terrain structures based on proposed simulation method. Based on coherence evaluation of Figure 5 and RMSE studies, performance of proposed simulation method shows significant improvement by incorporating multilook technique. Figure 5 plot of interferometric phase versus coherence coefficient is matching with the theoretical result of multilook phase distribution as Figure 3. Both showing that the standard deviation decreases as coherence coefficient and number of look increases. For comparing the final outcome with the actual value of the simulated terrain structure, we could use root mean square error to assess the performance of this simulation method. Such metric are used for comparison of Table 2 on multilook technique. For terrain hill & sinking holes structure, the multilook technique has reduce 2.04 RMSE. Likewise, 1.08 RMSE has been improved in fringe structure. Due to high destructive simulated outcome of spiral, its RMSE result is not appropriate to be taken into multilook studies.

Table 2: Root Mean Square Error of InSAR Simulation

Terrain Structure Type	Terrain hill & sinking holes	Fringe	Spiral
Single Look	8.28	5.18	>100
Multi-Look (4 look)	6.24	4.10	>100

Table 3: Comparison of InSAR Software

Features	Aforementioned Simulation techniques (Xu and Cumming, 1997), (Li et al., 2005), (Li and Yang, 2009)	Processing Software e.g GMTSAR, Doris	Proposed Simulation Method
Artificial input data	Yes	No	Yes
Noise simulation	Yes	No	Yes
Denoising and phase unwrapping	No	Yes	Yes
Less complexity	Yes	No	Yes

Our simulation results have demonstrated the complete InSAR processing. We also reviewed and compared existing simulation approaches of InSAR processing software with our proposed method as table 3.

5. Conclusion

The modelling and processing of InSAR are investigated in this paper. Besides, an efficient simulation method is proposed and demonstrated. The simulation results of artificial terrain structures and the process of interferogram, unwrapping and denoising terrain maps are presented. Such methods, also, can be great valuable for performance analysis and advance 2D phase-unwrapping research of InSAR system.

Acknowledgement

This work are supported by JICA (Japan International Coorperation Agency) and JST under SATREPS Project, Ministry of Education Malaysia (MOE) under Grant 203/PJJAUH/6711279. The contributions of aforementioned parties are sincerely appreciated and gratefully acknowledged.

References

Bamler, R. and Hartl, P., 1998, Synthetic Aperture Radar Interferometry, *Inverse Problems*, 14, 1-54.

Gens, R., 1999, SAR Interferometry: Software, Data Format, and Data Quality, *Photogrammetric Engineering and Remote Sensing,* 65(12), 1375-1378.

Ghighlia, D. C. and Pritt, M. D., 1998, Two-Dimensional Phase Unwrapping: Theory, Algorithms, and Software, 1st edition, (New York: Wiley-Interscience).

Lee, J. S., Dewaele, P., Wambacq, P., Oosterlinck, A. and Jurkevich, I., 1994, Speckle Filtering of Synthetic Aperture Radar Images - A Review, *Remote Sensing Reviews*, Vol. 8, 313-340.

Li, W. Q., Li, J. W. and Chen, J., 2005, Fast Simulation of Complex Image for Interferometric SAR, *Journal of Beijing University of Aeronautics and Astronautics*, 31(1), 31-35.

Lin, L. and Yang, W., 2009, Modeling and Simulation of Single-Look Complex Images for Distributed Satellite borne Interferometric Synthetic Aperture Radar, *Image and Signal Processing, 2009. CISP '09. 2nd International Congress*.

Matlab help file [Online]. Available: http://www.mathworks.com/help/images/ref/wiener2.html

Munther, G. and Francise, L., 2013, *Two Dimensional Phase Unwrapping Problem,* [Online].Available: https://www.ljmu.ac.uk-/~/media/files/ljmu/about-us/faculties-and-schools/tae/geri/two_dimensional_phase_unwrapping_finalpdf.pdf?la=en

Richards, M. A., 2007, A Beginner's Guide to Interferometric SAR Concepts and Signal Processing, *IEEE A and E Systems Magazine*, 22(9), 5-29.

Rosen, P. A., Hensley, S., Joughin, I. R., Madsen, S. N., Rodriguez, E. and Goldstein, R. M., 2000, Synthetic Aperture Radar Interferometry. *Proceeding of IEEE*, 88(3), 333-382.

Xu, W. and Cumming, I., 1997, Simulator for Repeat-Pass Satellite InSAR Studies, *Proceeding of International Geoscience and Remote Sensing Symposium 1997*, 1704-1706.

Zebker, H. A. and Lu, Y. P., 1998, Phase Unwrapping Algorithms for Radar Interferometry—Residue-cut, Least-squares, and Synthesis Algorithms. *Journal of the Optical Society of America*, 15(3), 586–598.